ORIGINAL ARTICLE

Comparison of two endovascular treatments of a stenosed arteriovenous fistula: balloon-angioplasty with and without stenting

Iolanda Decorato, Zaher Kharboutly, Cécile Legallais, Anne-Virginie Salsac

Biomechanics and Bioengineering Laboratory (UMR CNRS 7338), Université de Technologie de Compiègne, Compiègne - France

Purpose: *Arteriovenous fistulas (AVFs) are created in patients to enable a permanent vascular access for hemodialysis. The AVF causes changes in the hemodynamic conditions leading to possible complications, stenoses being the most common one. Our objective was to compare the effect of treating the stenosed AVF by balloon-angioplasty, whether followed or not with stenting.*
Methods: *We considered an AVF presenting an 60% arterial stenosis and simulated the two endovascular treatments using an implicit approach. We then simulated the fluid-structure interactions (FSI) within (i) the patient-specific stenosed AVF, (ii) the AVF after angioplasty, and (iii) the AVF after angioplasty plus stenting with ANSYS Workbench.*
Results: *We show that a self-expandable stent does not modify the curvature of the vessel after angioplasty; it only increases the local Young modulus of the stented wall by an order of magnitude. The results of the FSI simulations indicate that the two treatments induce the same hemodynamic conditions: they both reduce the pressure difference across the stenosis, while maintaining the flow distribution downstream of the stenosis. The venous flow rate that has to be guaranteed for hemodialysis is unaltered. Thanks to its large axial flexibility, the self-expandable stent causes at maximum a three-fold increase in the internal wall stresses at peak systole as compared to angioplasty alone.*
Conclusions: *By maintaining the vessel lumen shape over time, the stent is likely to reduce the risk of restenosis that can otherwise occur after balloon-angioplasty because of the viscoelastic recoil of the vessel.*

Keywords: *Arteriovenous fistula, Stenosis, Balloon angioplasty, Stent, Hemodynamics, Fluid-structure interactions*

INTRODUCTION

Hemodialysis is the therapy typically adopted for end-stage renal disease patients, while waiting for kidney transplantation (1). It consists in supplying the kidney filtering function through a partial extracorporal circulation. Blood circulation to the hemodializer is achieved through a permanent vascular access. Various types of vascular access exist. One option is to create an arteriovenous fistula (AVF), which connects a vein onto an artery (2). AVFs have a low complication rate when compared to other options, such as grafts and central venous catheters (3-4). But fistulas can be affected by different pathologies over time, one of them being the formation of stenoses.

Stenoses result in the reduction of the vascular lumen and lead to an increase in hydraulic resistance. They are

typically caused by neo-intimal development or athero-sclerotic plaque formation in regions of altered hemody-namics (5-6). Such flow conditions prevail, for instance, in the outflow vein of the fistula. But end-stage renal disease patients also present several comorbidities, such as hypertension and calcium-phosphate imbalance, which can lead to the development of calcified atherosclerotic plaques (7-8). The combined effects of altered hemody-namics and vascular wall calcification explain why patients in hemodialysis may be affected by stenoses at multiple sites along the vascular tree.

In the case of AVFs, stenosis are typically treated, when they occlude more than 50% of the lumen (9) or when they induce a local pressure difference ΔP above 5 mmHg (10). The most common treatment option is balloon-angioplasty. A balloon folded in a catheter is inserted endovascu-larly, guided across the vasculature up to the stenosis and inflated to restore the vessel lumen. Balloon-angioplasty has been proven to lengthen the period of fistula function-ality (10-12).

Another endovascular treatment consists in deploying a stent across the lesion (11). Stenting usually follows the preliminary expansion of the stenosis by balloon-an-gioplasty. Two types of self-expandable stents are used to treat AVF stenoses: stents in Nitinol (e.g. SMART®, Cordis, Miami, FL, USA) (13) or in stainless steel (e.g., Wallstent®, Boston Scientific, Natick, MA, USA) (14). The efficacy of stenting has been questioned since the late 80s (14) and it has only recently been proven to be more effective than balloon-angioplasty alone (13,15).

The objective of the study is to evaluate and compare the effects of both endovascular treatments on the hemodynamics and wall mechanics. The fluid-structure interactions (FSI) are simulated within the fistula before and after each treatment and compared to the untreated case. For the stented vessel, we have first searched for the mechanical behavior of the stented arterial section and determined its equivalent stiffness. For the FSI simu-lation in the stented AVF geometry, we have modeled the presence of the stent by imposing the equivalent stiffness to the stented portion of the artery. The local influence of the presence of the stent struts is thus neglected. The paper is structured as follows: after detailing the numerical methods, we analyze the influence of the two treatments on the vessel shape, hemodynamics and internal stresses and finally discuss their clinical conse-quences.
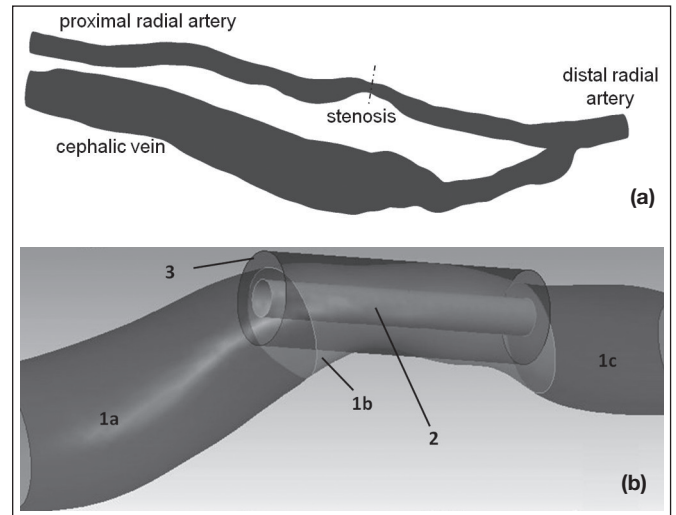
Fig. 1 - *(a) Geometry of the patient-specific fistula reconstructed from medical images. (b) Zoom on the stenosed region when both angioplasty and stenting are modeled. 1: artery, 2: angioplasty bal-loon, 3: stent*

MATERIALS AND METHODS

AVF, balloon and stent geometries

We consider a patient-specific mature side-to-end radio-cephalic AVF presenting an 60% stenosis on the arterial side (Fig. 1a). The images have been obtained by com-puted tomography (CT) scan angiography at the Polycli-nique St Côme (Compiègne, France) in conformity with the ethical standard at the time of measurement (16). The geometry of the vascular lumen is segmented and recon-structed. The vascular wall is then extracted and divided into three zones – the healthy artery, the stenosed arterial portion and the vein – in order to set different mechanical properties for each portion.

The angioplasty balloon is modeled as a cylindrical surface (Fig. 1b - '2'). The cylinder is created within ANSYS Geom-etry Interfaces (ANSYS, Canonsburg, PA, USA). Its length is 15 mm and its diameter 1 mm.

The stenting treatment is modeled with a self-expandable braided stent, the stainless steel Wallstent® wirestent (Boston Scientific, Natick, MA, USA), as it is one of the most used stents to treat stenosed fistulas. It is modeled as a tubular structure made of 24 separate wires spiraling clockwise and anti-clockwise. The stent ('3' in Fig. 1b) is created with the software PyFormex (©Benedict Verhegge, Ghent University, Belgium) with a length of 12 mm and a diameter of 4.2 mm, which is the diameter of the inlet
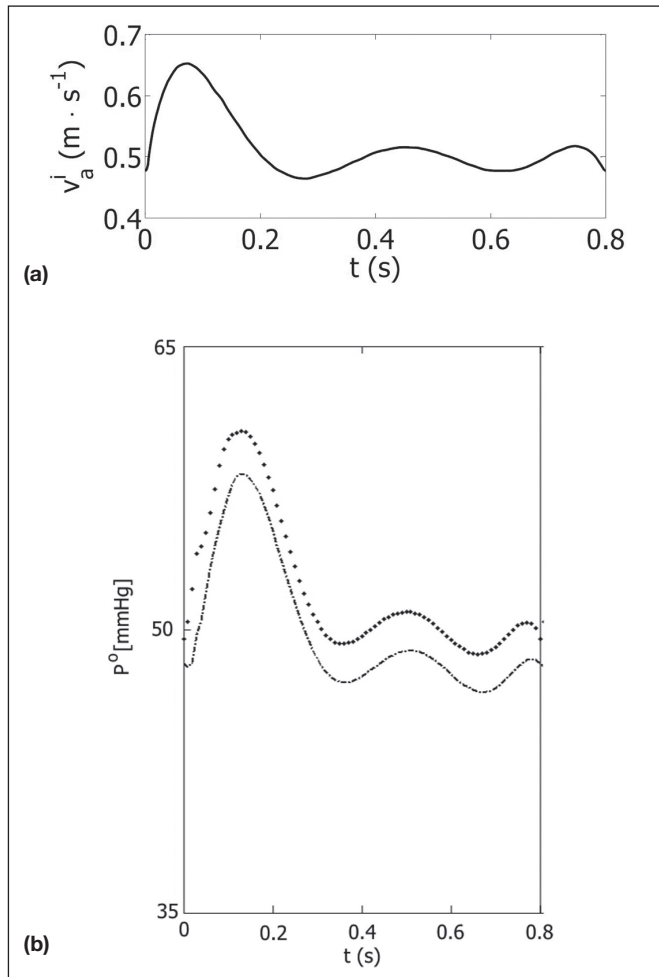
Fig. 2 - (a) *Flat time-dependent velocity profile v^i_a prescribed at the inlet of the proximal radial artery.* **(b)** *Arterial pressure profile P^o_a (dotted line) and venous pressure profile P^o_v (dot-mark line).*

artery upstream of the stenosis. The initial diameter of the stent is equal to the size that it has after deployment, since it is a self-deployable stent.

Mesh generation

The lumen of the AVF is meshed in ANSYS T-Grid by extrusion from the triangulation of the inflow lateral surface. The mesh is made of a hybrid grid of linear elements with prismatic elements in the boundary layer and tetrahedrons in the vessel core (17). The vascular wall is meshed with a monolayer of shell elements starting from the nodes of the lateral surface of the AVF lumen. This condition ensures that the fluid and solid domains share the same nodes at the interface. Different mesh sizes were created to study the con-

vergence of the numerical method. The present results were obtained with a 784 000-element mesh, for which the maximum error on the velocity magnitude and wall shear stresses is less than 1% and the results are grid-independent.

The arterial and venous wall thicknesses were taken from the literature, as no direct measurement was possible *in vivo*. The vein is modeled with the typical thickness of a cephalic vein prior to AVF creation (0.4 mm), since Corpataux et al (18) showed that it tends to remain constant during fistula maturation. The artery is assumed to have a thickness of one-tenth its inlet diameter, i.e. 0.6 mm (19).

The balloon is meshed with linear triangular shell elements using ANSYS Workbench Platform. To be exported, the stent has to be meshed in Pyformex. The hexahedral mesh is generated with the sweep method. However, the quality of the elements is not sufficient for simulations in ANSYS. The 24 wires are therefore imported in ANSYS and re-meshed with tetrahedrons with the default sweep patch-conforming algorithm.

Rheological and mechanical properties

Blood is assumed to be an isotropic, homogeneous, non-Newtonian fluid that follows the Casson model. The apparent viscosity μ is given by

$$\sqrt{\mu} = \sqrt{\tau_0 / \gamma} + \sqrt{K},$$

where γ is the shear rate, τ_o the yield stress and K the consistency. The model parameters have been adjusted to fit experimental results at low shear rates:

$\tau_o = 4 \times 10^{-3}$ Pa, $K = 3.2 \times 10^{-3}$ Pa.s (20). Blood density is set to 1050 kg.m^{-3}

Apart from the stenosed arterial region, we hypothesize that the vascular walls of the vein and artery are both made of a homogeneous, incompressible, hyperelastic material. They are assumed to follow the 3rd-order Yeoh model (21). The artery (Fig. 1b - '1a' and '1c') is modeled as more compliant than the vein, which is typical in AVFs. Since no measurements of the wall mechanical properties have ever been conducted on an AVF, the law constants are obtained by best-fitting stress-strain curves from measurements on a healthy artery and on a post-phlebitic vein (see (22) for more details). The stenosed part of the artery (Fig. 1b - '1b') is modeled as viscoplastic with a Maxwell constitutive law. The law parameters are set to retrieve the same stiffness as the healthy arterial wall at small

TABLE I - VALUES OF THE MECHANICAL PROPERTIES OF THE BALLOON AND STENT

	Balloon	Stent
p	1000 kg.m^{-3}	7999 kg.m^{-3}
E	9×10^8 Pa	2×10^9 Pa
v	0.3	0.3

deformation and to fit the data of Maher et al (23) at large deformation. This choice ensures continuity of the mechanical properties at the interface between the stenosed and non-stenosed segments.

The balloon and stainless steel stent are modeled as linear elastic materials. The mechanical properties indicated in Table I are those of stainless steel for the stent and those indicated in (24) for the balloon. We have imposed a Poisson coefficient $v = 0.3$ to guarantee numerical convergence.

Simulation of balloon-angioplasty

The opening of the balloon is simulated using ANSYS Structural Analysis software. The balloon is first positioned unfolded across the arterial stenosis without any contact with the wall. It is inflated by imposing a linearly increasing internal pressure with a maximum pressure of 5.1 bar. During opening, the balloon comes into contact with the artery. The contact is supposed to be frictionless (25) and is solved using the augmented-Lagrange method. At each instant of time, the structural simulation consists in finding the mechanical equilibrium between the deformable artery and the elastic balloon using the implicit approach. When the maximum pressure is reached, the balloon is deflated with a linearly decreasing pressure. The degree of residual stenosis is equal to 20% after treatment.

Simulation of balloon-angioplasty followed with stent positioning

Balloon-angioplasty followed by stent deployment is modeled with ANSYS Structural Analysis software in a two-step implicit simulation. The balloon inflation is first simulated as described previously, while keeping the stent inactivated (i.e., transparent to the balloon and vessel). The stent is only activated at the end of this first step. The second step corresponds to the balloon defla-

tion, during which the arterial wall comes into contact with the stent. The simulation solves for the mechanical equilibrium of the stent within the artery. The equilibrium shapes of the artery and stent are function of their mechanical properties. We define the contact between the artery and stent as frictional following the Coulomb theory. The friction coefficient is equal to 4.5×10^{-2} (24). Conversely, no contact is defined between the stent and the balloon.

Evaluation of the equivalent stiffness of the stented artery

The equivalent stiffness of the stented artery is determined following an inverse analysis approach using ANSYS-Structural. To do so, two simulations of vessel inflation are run: one with the stent present in the artery (reference case) and the other one with a bare vessel. In both cases, the vessel geometry is the one of the artery after angioplasty plus stenting.

The deformation of the stented artery is obtained by imposing a linearly increasing pressure in the lumen in an implicit structural simulation. The contact between the artery and the stent is configured to be bonded, which guarantees that the artery and stent deform together under the imposed pressure. We then search which mechanical properties to provide to the bare vessel wall to obtain the same deformation during inflation as the stented artery.

Simulation of the fluid-structure interactions

The fluid-structure interactions are simulated implicitly in the geometries obtained after balloon-angioplasty with and without stenting. The numerical method has been described in details in (22). Briefly, we couple implicitly the fluid and solid domains in ANSYS Workbench Platform. The finite element structural solver uses a Lagrangian multiplier-based mixed deformation-pressure numerical scheme (u-P formulation). The simulation is performed assuming large displacements. The fluid solver is based on the Rhie-Chow interpolation method to calculate the velocity field implicitly (26). We consider the atmospheric pressure as reference pressure and neglect gravity. The fluid-structure interactions are solved iteratively using the arbitrary Lagrangian-Eulerian formulation.

Iterations are repeated within each time-step until all the field equations have converged and the coupling conditions are satisfied. Each FSI simulation is run over six consecutive

cardiac cycles, with a time step equal to 5×10^{-3} s for both the fluid and the solid solver.

As boundary conditions, we impose (*i*) 0-rotation and 0-translation at the vascular wall extremities; (*ii*) the time-dependent velocity profile measured on the patient at the inlet - systolic Reynolds number of 1230, time-averaged Reynolds number of 1020, Womersley number of 4 (Fig. 2a); (*iii*) time-dependent pressure outlet profiles (Fig. 2b). The issue is that no patient pressure value can be obtained *in vivo*, as pressure measurement is invasive. We have therefore opted to impose the same inlet flow condition in the three configurations: we can thus evaluate the consequences of the endovascular procedure immediately after treatment, i.e., prior to any systematic change and adaptation. The outlet pressures were obtained conducting a rigid-wall simulation in ANSYS CFX, applying Windkessel models at the two outlets. The constants of the Windkessel model are tuned following the method described in Decorato et al (17): they are obtained by imposing the measured value of the flow split between the arterial and venous outlets (30-70%, respectively) and prescribing an expected time-averaged inlet pressure.

RESULTS

Post-treatment AVF geometry

A residual stenosis of 20% is achieved in both the stented and non-stented cases. Figure 3 shows the stenosed artery before treatment (a), after balloon-angioplasty (b) and after balloon-angioplasty plus stenting (c). The initial position of the balloon is indicated by the cylinder in Figure 3a. The comparison of Figs. 3b and 3c shows that the geometry of the vessel is almost unchanged by the presence of the stent. No clear change in the vessel curvature can be noticed.

Equivalent stiffness of the stented artery

Figure 4 compares the stress-strain curves for the stented and non-stented artery. It shows that, when stented, the vessel obeys the Hooke's law. The linear elastic mechanical behavior of the stent therefore prevails over the viscoplastic behavior of the artery. The equivalent Young modulus E_{eq} of the stented vessel is 437 MPa, which is about 9 times larger than the stenosed artery at small
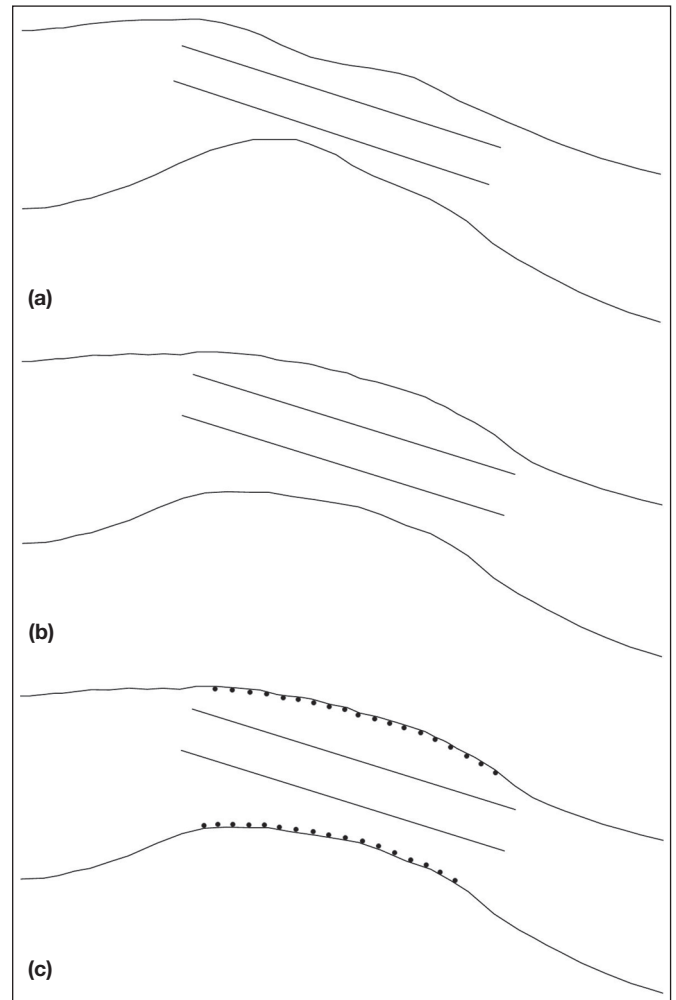

Fig. 3 - *Geometry of the afferent artery of the fistula (b) after treatment (b) after balloon-angioplasty and (c) after balloon-angioplasty with stenting. Both post-treatment cases present a residual stenosis equal to 20%.*

deformations. The Wallstent® (Boston Scientific, Natick, MA, USA) therefore increases locally the vessel stiffness of the vessel after deployment. The value E_{eq} is imposed to the stenosed region of the artery in the FSI simulation of the stented geometry.

Hemodynamics
Influence of balloon-angioplasty

In order to evaluate the influence of the stenosis treatment, we have detailed the values of a few key hemodynamic parameters provided by the FSI simulations (Tab. II).
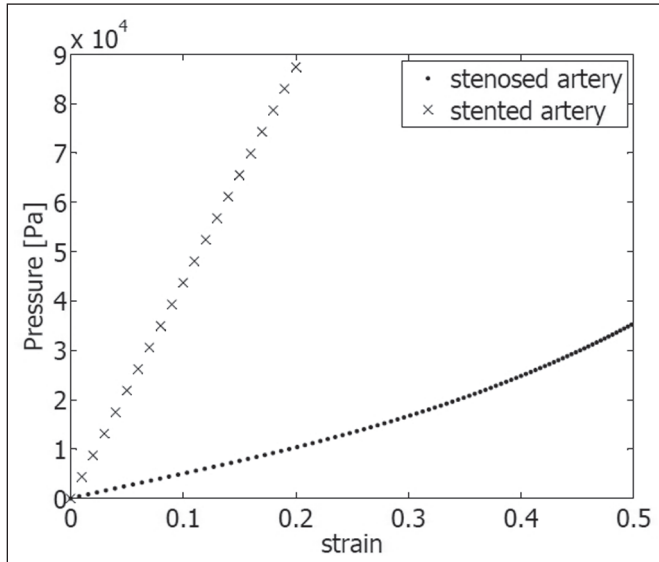
Fig. 4 - *Pressure-strain relationship of the stented artery (cross symbol) as compared to the patient-specific non-treated case (dot symbol).*

TABLE II - COMPARISON OF THE MOST RELEVANT HE-MODYNAMIC PARAMETERS AFTER BALLOON-ANGIOPLASTY WITH AND WITHOUT STENTING VERSUS THE NON-TREATED CASE

	60%-Stenosis	Angioplasty	Angioplasty + Stent
v_{max} (m.s^{-1})	2.12	1.89	1.90
$\overline{WSS}_{stenosis}$ (Pa)	27.0	12.0	12.4
$\overline{Q}_v$ (ml.min^{-1})	779.0	772.0	772.2
ΔP (mmHg)	11.70	4.92	4.95

Comparing the results before and after balloon-angioplasty, one can observe that the treatment has a significant effect on the stenosis region. It reduces the maximum velocity at the stenosis V_{max} by about 10%, which induces a 50% decrease in the wall shear stresses $\overline{WSS}_{stenosis}$.

The pressure distribution along the AVF is provided in Figure 5 before treatment. Angioplasty also leads to a 60% decrease in the pressure difference across the stenosis ΔP (Table II). For a residual degree of stenosis of 20%, the pressure difference is below 5 mmHg, indicated in the literature as the threshold value for treatment (10). The treatment can thus be regarded as successful.
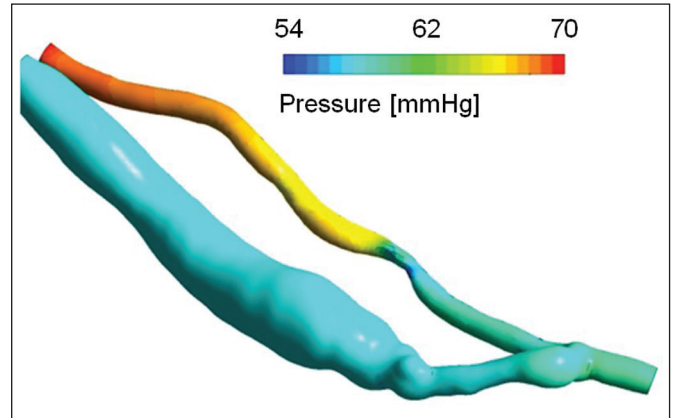
Fig. 5 - *Distribution of the systolic pressure along the fistula.*

Table II shows that the venous flow rate Q_v remains unchanged. Indeed, we find that angioplasty hardly impacts the hemodynamics downstream of the stenosis.

Additional effect of stenting

The sole influence of stenting can be obtained by comparing the FSI results, when angioplasty is followed or not by stenting (Tab. II). Hardly any difference can be noticed between the two treatments. They both lead to the same maximum velocity V_{max} and wall shear stresses $\overline{WSS}_{stenosis}$ at the stenosis. They engender the same flow distribution between the arterial and venous outlets, as shown by the similar values of venous flow rate Q_v. The pressure drop at the stenosis ΔP is neither affected by stent positioning: the treatment of the stenosis can be considered as successful in both cases, since ΔP remains each time below 5 mmHg.

Internal wall stresses

The local strain and internal wall stresses are evaluated after balloon-angioplasty with and without stent positioning and compared to the untreated case. The internal stresses are evaluated using the maximum component of the Cauchy stress tensor σ_{max}. They are compared to the mean stress in the healthy artery σ_{art}, which is a good estimate of the baseline stress. Our objective is to see whether the endovascular treatments cause a departure of the internal stress from their baseline value. The vessel pre-stress has thus been neglected.

**TABLE III -** SPATIAL-AVERAGED VALUES OF THE STRAIN AND NORMALIZED STRESSES AT THE STENOSIS AT PEAK SYSTOLE

	60%-Stenosis	Angioplasty	Angioplasty + Stent
Strain	15%	9%	3%
$\sigma_{max} / \sigma_{art}$	1.1	5	14

In Table III, we compare the spatial-averaged strain and stresses provided by the three FSI simulations at peak systole in a region around the stenosis throat (10 mm in length).

We observe that the maximum strain decreases by 40% after balloon-angioplasty and by 80% after balloon-angioplasty with stenting. Conversely, the normalized internal stress σ_{max} / σ_{art} at the stenosis results to be 5 times larger after angioplasty alone and 14 times larger, when a stent is deployed.

In Figure 6, we compare the time-averaged distribution of the normalized internal stress $\sigma_{max}/\sigma_{art}$ after the two treatments. After balloon-angioplasty, the stenosis region is subjected to an internal stress σ_{max}, which is up to 11 times larger than the baseline value σ_{art}. This residual stress is due to the permanent plastic deformations that occur within the vessel wall during balloon inflation. The positioning of a stent further increases the residual stress. The stress σ_{max} can be as large as 19 times the baseline value within the stented region. It is a consequence of the increase in vessel wall stiffness induced by the stent. Within the cephalic vein the stress distribution is the same before and after the treatment: it is about twice the baseline stress in the artery.

Away from the stenosis, the stress σ_{max} decreases and regains the values observed in the healthy artery. In the region upstream of the stenosis, the baseline stresses are completely recovered over a distance of 1.2 mm in the case of the simple balloon-angioplasty and of 2.5 mm in the case of stenting (Fig. 6). The gradient of the internal wall stresses space-averaged across the stenosed region remains of the same order of magnitude as after balloon-angioplasty: it is at maximum tripled following stenting. The stent locally causes a larger stress gradient at the interface between the stented and non-stented portions of the artery with a 3.5-fold increase. Downstream of the stenosis, the baseline stress value is recovered after a distance of 1.3 mm after both treatments.
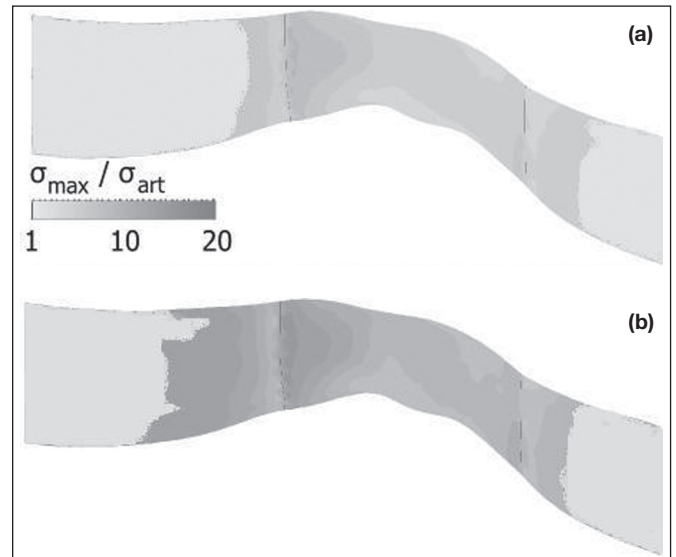
Fig. 6 - *Time-averaged distribution of the maximum component of the Cauchy stress tensor σ_{max} normalized by the mean stress in the healthy artery σ_{art} in the stenosis region: after balloon-angioplasty **(a)**; after balloon-angioplasty and stent positioning **(b)**.*

DISCUSSION

The results of the study show that positioning a self-expandable stent (e.g., Wallstent®) after balloon-angioplasty has a negligible effect on the vascular geometry. The shape and curvature of the vessel are hardly modified. The stent does not straighten the vessel, which indicates a small bending rigidity of the general structure. This is coherent with what has been found by Duerig and Wholey (27). The wirestent device is designed to have a high radial stiffness to prevent the re-occlusion of the vessel, and a large axial flexibility to follow the curvature of the vasculature after the deployment.

The inverse analysis provides a quantitative proof of what is guessed from the shape of the stented wall. The equivalent stiffness of the stented artery is only about 10 times larger than the bare artery (i.e., non-stented). It corroborates the *in vivo* results obtained by Vernhet et al for Wallstent® stents implanted in a rabbit abdominal aorta (28). The relatively small increase in the local vascular stiffness is due to the smaller rigidity of self-expandable stents as compared to balloon-expandable ones (27). Self-expandable stents also have the advantage to subject the vascular wall to an expansion force sustained over time. They do not suffer from radial recoil, as it can be the case for balloon-expandable

stents (27, 29). Another advantage is the relatively small trauma caused to the endothelial cells by the stent deployment, in contrast to balloon-expandable stents (25).

The comparison of the results of the fluid-structure interaction simulations shows that the two treatment options have an equivalent immediate effect on the hemodynamics both locally at the stenosis and globally in terms of distal flow split. These results are supported by recent clinical studies (15). The hemodynamics is therefore hardly influenced by the local increase in stiffness of a portion of the vasculature.

The fact that the venous outflow $\overline{Q}_v$ keeps the value it had before treatment is particularly relevant for hemodialysis: the fistula remains functional despite the presence of an arterial stenosis. This is very different to the case of venous stenoses, which reduce the venous outflow. Arterial stenoses, however, induce a large pressure drop in the afferent artery. It is not clear which effect the latter has on the overall blood circulation. Some believe that the pressure drop is responsible for a higher pressure upstream of the AVF and thus for an increased cardiac work. In this hypothesis it is advisable to treat any stenosis as early as possible to reduce the pressure drop and thus the risk of heart failure. Indeed, all hemodialyzed patients are particularly vulnerable to premature cardiac disease and failure, since the fistula creates a direct connection between arteries and veins and thus decreases the downstream vascular resistance (10, 30, 31). Another hypothesis could be that the stenosis actually has a protecting effect: by increasing the hydraulic resistance and limiting the flow in the radial artery, it decreases the venous pressure. Whole-body flow simulations could shed light on this question.

When considering the influence of the two treatments on the wall mechanics, we observe a larger difference than on the hemodynamics. The study has shown that residual stresses build up within the vascular wall following balloon-angioplasty: the internal wall stresses at the stenosis throat are, on average, five times the baseline value at peak systole (Tab. III). Stenting causes an increase in the maximum internal wall stresses and in their spatial gradient, which is associated with the induced increase in vessel wall rigidity. In the case of a Wallstent® stent, the increase is moderate (at maximum they are tripled). There should therefore be a limited risk of in-stent restenosis. Restenosis has been shown to mainly appear in the case of axially rigid balloon-expandable stents (32): the

latter can cause local alteration in wall shear stresses in the regions upstream and downstream of the stent, which is prone to neointima proliferation (32). But contrary to balloon-expandable stents, the self-expandable wirestent Wallstent® has a high axial flexibility.

In clinics it has been observed that balloon-angioplasty alone often fails because of the viscoelastic recoil of the vessel within 6 to 12 months after the treatment (15). It has been proven recently that the additional use of stenting renders balloon-angioplasty more efficient, especially in the long term (13, 15). From the present results, one can hypothesize that it may due to the fact that the stent maintains the vessel open. The beneficial impact of the stent is likely to be small immediately after treatment and to increase in the months following treatment, when the bare vessel experiences natural recoil.

FSI simulations cannot model the viscoelastic recoil and predict the long-term response of the vascular wall. In the future it would be interesting to build a model of the evolution of the vessel, taking into account the endothelial response to hemodynamic solicitations as well as the wall response to altered internal stresses.

CONCLUSIONS

We have implicitly simulated the treatment of an AVF presenting an 60% arterial stenosis by balloon-angioplasty with and without stent positioning. We have shown that implanting a self-expandable stent has the advantage of preserving the curvature of the treated vessel and causing a moderate increase in the local stiffness of the artery. Comparing the flow conditions predicted by the FSI simulations, we have found that the two treatments are equivalent. They preserve the functionality of the fistula, as none of them perturbs the flow distribution in the AVF; they both reduce the pressure difference across the stenosis below its critical threshold value ($\Delta P \leq 5$ mmHg). The comparison of the internal wall stresses after the two treatment options indicates that stent positioning leads to a maximum three-fold increase in the wall internal stress σ_{max} at the stenosis throat. This is moderate enough for in-stent restenosis to be unlikely to develop over time. The beneficial effect of stenting observed in clinics must come from the fact that the stent prevents the natural elastic recoil of the vessel after angioplasty and therefore the occurrence of restenosis.

Address for correspondence:
Anne-Virginie Salsac
Biomechanics and Bioengineering Laboratory
(UMR CNRS 7338)
Université de Technologie de Compiègne
CS 60319
60203 Compiègne, France
anne-virginie.salsac@utc.fr

REFERENCES

1. Horl WH, Koch KM, Ronco C, Winchester JF. Replacement of Renal Function by Dialysis. Kluwer Academic Publishers; 2004.
2. Konner K, Nonnast-Daniel B, Ritz E. The arteriovenous fistula. J Am Soc Nephrol. 2003;14(6):1669-1680.
3. Malovrh M. How to increase the use of native arteriovenous fistulae for haemodialysis. Prilozi. 2011;32(2):53-65.
4. Torreggiani M, Scaramuzzi ML, Manini A, et al. Hemodialysis vascular access: everything you always wanted to know about it (but were afraid to ask). J Nephrol. 2013;26(5):836-847.
5. Van Tricht I, De Wachter D, Tordoir J, Verdonck P. Hemodynamics and complications encountered with arteriovenous fistulas and grafts as vascular access for hemodialysis: a review. Ann Biomed Eng. 2005;33(9):1142-1157.
6. Lee T, Roy-Chaudhury P. Advances and new frontiers in the pathophysiology of venous neointimal hyperplasia and dialysis access stenosis. Adv Chronic Kidney Dis. 2009;16(5):329-338.
7. Braun J, Oldendorf M, Moshage W, Heidler R, Zeitler E, Luft FC. Electron beam computed tomography in the evaluation of cardiac calcification in chronic dialysis patients. Am J Kidney Dis. 1996;27(3):394-401.
8. Perkovic V, Hunt D, Griffin SV, du Plessis M, Becker GJ. Accelerated progression of calcific aortic stenosis in dialysis patients. Nephron Clin Pract. 2003;94(2):c40-c45.
9. Asif A, Gadalean FN, Merrill D, et al. Inflow stenosis in arteriovenous fistulas and grafts: a multicenter, prospective study. Kidney Int. 2005;67(5):1986-1992.
10. Forauer AR, Hoffer EK, Homa K. Dialysis access venous stenoses: treatment with balloon angioplasty—1- versus 3-minute inflation times. Radiology. 2008;249(1):375-381.
11. Ozyer U, Harman A, Yildirim E, Aytekin C, Karakayali F, Boyvat F. Long-term results of angioplasty and stent placement for treatment of central venous obstruction in 126 hemodialysis patients: a 10-year single-center experience. AJR Am J Roentgenol. 2009;193(6):1672-1679.
12. Kim YC, Won JY, Choi SY, et al. Percutaneous treatment of central venous stenosis in hemodialysis patients: long-term outcomes. Cardiovasc Intervent Radiol. 2009;32(2):271-278.
13. Hatakeyama S, Toikawa T, Okamoto A, et al. Efficacy of SMART stent placement for salvage angioplasty in hemodialysis patients with recurrent vascular access stenosis. Int J Nephrol. 2011;2011:464735.
14. Zollikofer CL, Antonucci F, Stuckmann G, Mattias P, Brühlmann WF, Salomonowitz EK. Use of the Wallstent in the venous system including hemodialysis-related stenoses. Cardiovasc Intervent Radiol. 1992;15(5):334-341.
15. Chan MR, Bedi S, Sanchez RJ, et al. Stent placement versus angioplasty improves patency of arteriovenous grafts and blood flow of arteriovenous fistulae. Clin J Am Soc Nephrol. 2008;3(3):699-705.
16. Kharboutly Z, Fenech M, Treutenaere JM, Claude I, Legallais C. Investigations into the relationship between hemodynamics and vascular alterations in an established arteriovenous fistula. Med Eng Phys. 2007;29(9):999-1007.
17. Decorato I, Salsac A-V, Legallais C, Ali-Mohammadi M, Diaz-Zuccarini V, Kharboutly Z. Numerical simulation of the treatment of an arterial stenosis in an arteriovenous fistula by balloon-angioplasty. Cardiovascular Engineering and Technology. In press.
18. Corpataux JM, Haesler E, Silacci P, Ris HB, Hayoz D. Low-pressure environment and remodelling of the forearm vein in Brescia-Cimino haemodialysis access. Nephrol Dial Transplant. 2002;17(6):1057-1062.
19. Gutierrez MA, Pilon PE, Lage SG, Kopel L, Carvalho RT, Furuie SS. Automatic measurement of carotid diameter and wall thickness in ultrasound images. Comput Cardiol. 2002;29:359-362.
20. Merrill EW, Pelletier GA. Viscosity of human blood: transition from Newtonian to non-Newtonian. J Appl Physiol. 1967;23(2):178-182.
21. Yeoh O. Some forms of the strain energy function for rubber. Rubber Chem Technol. 1993;66:754-771.
22. Decorato I, Kharboutly Z, Vassallo T, et al. Numerical simulation of the fluid structure interactions in a compliant patient-specific arteriovenous fistula. Int J Numer Method Biomed Eng. 2014;30(2):143-159.

23. Maher E, Creane A, Sultan S, Hynes N, Lally C, Kelly DJ. Inelasticity of human carotid atherosclerotic plaque. Ann Biomed Eng. 2011;39(9):2445-2455.

24. Gervaso F, Capelli C, Petrini L, Lattanzio S, Di Virgilio L, Migliavacca F. On the effects of different strategies in modelling balloon-expandable stenting by means of finite element method. J Biomech. 2008;41(6):1206-1212.

25. Gasser T, Holzapfel G. Finite element modeling of balloon angioplasty by considering overstretch of remnant non-diseased tissues in lesions. Comput Mech. 2007;40(1): 47-60.

26. Rhie C, Chow W. Numerical study of the turbulent flow past an airfoil with trailing edge separation. AIAA J. 1983;21: 1525-1532.

27. Duerig T, Wholey M. A comparison of balloon- and self-expanding stents. Minim Invasive Ther Allied Technol. 2002; 11(4):173-178.

28. Vernhet H, Juan J-M, Demaria R, Oliva-Laurairea M-C, Senac J-P, Dauzat M. Acute changes in aortic wall mechanical properties after stent placement in rabbits. J Vasc Interv Radiol. 2000;11:634-638.

29. Capelli C, Gervaso F, Petrini L, Dubini G, Migliavacca F. Assessment of tissue prolapse after balloon-expandable stenting: influence of stent cell geometry. Med Eng Phys. 2009;31(4):441-447.

30. Menno AD, Zizzi J, Hodson J, McMahon J. An evaluation of the radial arterio-venous fistula as a substitute for the Quinton shunt in chronic hemodialysis. Trans - Am Soc Artif Intern Organs. 1967;13(1):62-67. Available at ASAIO Journal. Accessed April 7, 2014.

31. Schwab SJ, Saeed M, Sussman SK, McCann RL, Stickel DL. Transluminal angioplasty of venous stenoses in polytetrafluoroethylene vascular access grafts. Kidney Int. 1987;32(3): 395-398.

32. Rogers C, Tseng DY, Squire JC, Edelman ER. Balloon-artery interactions during stent placement: a finite element analysis approach to pressure, compliance, and stent design as contributors to vascular injury. Circ Res. 1999;84(4):378-383.